ECS Solid State Letters, **1** (4) P60-P62 (2012)
2162-8742/2012/1(4)/P60/3/$28.00 © The Electrochemical Society

Side Wall Wetting Induced Void Formation due to Small Solder Volume in Microbumps of Ni/SnAg/Ni upon Reflow

Y. C. Liang,[a] C. Chen,[a,z] and K. N. Tu[b]

[a]*Department of Materials Science and Engineering, National Chiao Tung University, Hsinchu 30010, Taiwan*
[b]*Department of Materials Science and Engineering, University of California at Los Angeles, Los Angeles, California 90095-1595, USA*

A processing failure of void formation has been observed in 3D IC microbumps due to small solder volume. We prepared the sandwiched Ni/Sn2.3Ag/Ni microbumps with 4 μm and 11 μm thick solders and reflowed them at 260°C to study the mechanism of void formation in the processing. Due to the thin solder, intermetallic compound formation of Ni_3Sn_4 from the two interfaces of the solder joint can physically bridge each other. When that happens, the degree of freedom of motion in the direction normal to the interfaces is removed. Consequently, when the remaining molten solder is drained by side wall reaction, large voids form in the joint. This is a unique mode of processing failure because of the smaller and smaller volume of solder joints in the trend of miniaturization.
© 2012 The Electrochemical Society. [DOI: 10.1149/2.002204ssl] All rights reserved.

Manuscript submitted May 30, 2012; revised manuscript received July 13, 2012. Published August 22, 2012.

For high-density packaging in microelectronic industry, the three dimensional integrated circuits (3D IC) by vertically stacked silicon chips is expected to achieve higher performance than the conventional flip-chip technology. This is because in order to accomplish the multi-functional requirements for future generation electronics, interconnections with high input/output counts and fine pitch are needed. Therefore, fine pitch interconnections with through-silicon-vias (TSVs) of Cu vias for 3D IC of Si chips has been developed recently.[1] Microbump technology is required to join the vias between Si chips. Lead-free solder bumps about 10 μm in height and in diameter were adopted in microbumps.[2] In contrast with conventional flip-chip solder bumps, which have a height and diameter of 100 μm, a microbump has a much smaller solder volume, about 1000 times smaller. In the transition from flip chip technology to microbump technology, the solder volume change has caused new processing issues as well as reliability issue. For example, under the same reflow condition of time and temperature, a much larger volume fraction of intermetallic compounds (IMCs) is formed in microbumps. Because of the need to reduce the fraction of IMCs, a few microns thick Ni layer under-bump-metallization (UBM) has been coated at the surface of the Cu vias as a diffusion barrier.[3,4] Thus, the interfacial reactions between Pb-free solder and Ni UBM have attracted a great deal of attention. In this paper, we report a processing failure in the Ni UBM microbump.

In the literature, several reports have addressed the metallurgical reactions between Pb-free solders and Ni UBM in flip chip technology.[5–20] IMC of Ni_3Sn_4 forms, and the interfacial morphology of Ni_3Sn_4 depends on the reaction conditions and plays a crucial role in affecting the mechanical reliability of the solder joints.[3,17,18] How does the small solder volume in microbumps affect the morphology and growth kinetics of Ni_3Sn_4 requires a systematic study. Indeed very few literatures covered the topic.[21,22] It is expected that after a longer reaction time, the entire Pb-free solder can be transformed into IMC completely. In other words, the IMC from both sides of the solder joint joined to each other, and the joint became an IMC joint. In this study, we investigated the interfacial morphology of Ni_3Sn_4 IMC in a sandwiched structure of Ni/Sn2.3Ag/Ni microbump during various reflowing times at 260°C. The thickness of the solder between two Ni UBM layers is 4 μm and 11 μm. We observed very large void formation in the thinner solder joint during reflow.

Experimental

Sandwiched Ni/Sn2.3Ag/Ni microbumps were fabricated by joining two Ni/Sn2.3Ag samples as depicted in Figure 1. A layer of 0.1 μm thick Ti was deposited onto an oxidized Si wafer first to serve as an adhesion layer and followed by sputtering a Cu seed layer of 0.2 μm thick. After that, photolithography was employed to pattern cylinders of 100 μm in diameter for the electroplating of 3 μm Ni UBM and the Sn2.3Ag solder of three sets of thickness of 1 μm, 2 μm, and 10 μm. After electroplating of the Ni and the solder, the wafers were reflowed at 260°C for 1 minute (the first reflow) to ensure solder cap formation on the Ni. Then they were diced to be 2.3 × 2.3 mm Si chips. After that, one chip with 2 μm thick solder were flipped over and aligned with another chip. The schematic experimental setup is shown in Figure 1a. Then they were joined together at 260°C for 3 minutes (the second reflow) to form microbump solder joints with 4 μm thick solder. For comparison, microbump solder joints with 11 μm thick solder were also prepared by joining samples of 10 μm thick and 1 μm thick solder using the same method, as depicted in Figure 1b. The solder thickness was measured to be 4.2 ± 0.1 and 11.1 ± 0.2 μm for the two sets of samples, respectively. The pitch between adjacent microbumps was 200 μm. Metallurgical reactions were investigated for additional reflow at 260°C for 5, 10, 30, 60 and 120 minutes (the third reflow) on a hotplate, and then air-cooled at a cooling rate of 5°C/sec. We note here that the reflow time in this paper represents the total reflow time, which includes the 1 minute reflow after the electroplating, the 3 minutes reflow during joining the microbump samples, and the additional reflow to investigate the metallurgical reactions. Therefore, the reflow time under investigation is actually 4, 9, 14, 34, 64, and 124 minutes.

Cross-sections of the samples after the reflow were mechanically polished, and the microstructure of Ni_3Sn_4 IMC on the cross-sections was observed by scanning electron microscopy (SEM) with a back-scattered electron image (BEI) detector. The composition of the IMC was examined by energy dispersive spectroscopy (EDS). Growth of the IMC was quantified by calculation on the basis of image analysis software, which measured the IMC area on the cross-section and then divided by the interfacial length between the IMC and the Ni UBM.

Results and Discussion

For the 4 μm thick solder sample, the solder transformed completely to Ni_3Sn_4 IMC after reflow for 34 min, and many voids were observed in the middle of the joint. Figures 2a to 2c illustrate the cross-sectional SEM images of the sample after 4, 14, and 34 min respectively at 260°C. The as-joined microbump, shown in Figure 2a, has Ni_3Sn_4 IMC formed at both the top and the bottom interfaces. When the reflow time increased to 14 min, an obvious loss of the solder is seen in Figure 2b due to necking formation in the periphery of the joint. The loss of solder in the periphery of the microbump can be attributed to the out-flowing of the solder because of side wall wetting. The side wall of the cylindrical Ni UBM was a free surface and it can be wetted by the solder to form Ni_3Sn_4 IMC. It is a driving force for solder to flow out during reflow, which has been reported in previous literatures.[23,24] Actually, the sputtered Cu seed layers beneath

[z]E-mail: chih@mail.nctu.edu.tw

Downloaded on 2014-04-28 to IP 140.113.38.11 address. Redistribution subject to ECS terms of use (see ecsdl.org/site/terms_use) unless CC License in place (see abstract).

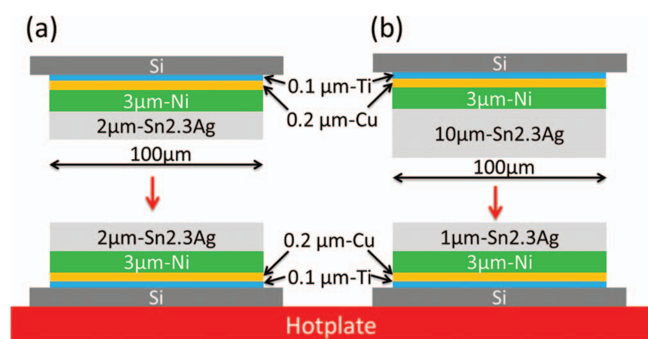

Figure 1. Schematic diagram for the microbump structures and the jointing setup used in this study. (a) 4-μm-thick solder sample; (b) 11-μm-thick solder sample.

the Ni UBM were consumed by the out-flowing solder too. After a 34 min reflow as shown in Figure 2c, many large voids were observed in the middle of the joint. This microbump was cross-sectioned by focused ion beam (FIB) to prevent artificial damage from mechanical polishing.

When the solder joint has a large volume as in flip chip technology, the side wall wetting will not lead to necking formation and void formation. But when the solder volume is small, void formation can occur. Three reasons may cause the serious void formation. First, Sn atoms may diffuse out to react with the Cu seed layer beneath the Ni UBM. Figures 3a to 3c represent the enlarged SEM images on the periphery of the joints for the samples shown in Figs. (2). It is clear that the Sn atoms diffuse along the lateral Ni_3Sn_4 IMC and migrate to the Cu seed layer to form $(Cu, Ni)_6Sn_5$ IMCs. As demonstrated in Fig. 3b, the IMCs at point B and point C were Ni_3Sn_4 confirmed by EDS; whereas the IMCs at point A and point D were detected to be Cu_6Sn_5 and $(Cu, Ni)_6Sn_5$, respectively. Furthermore, as shown in Fig. 3c, the IMCs at point F and point G were Ni_3Sn_4, and the IMCs at point E and point H were $(Cu, Ni)_6Sn_5$. Second, molar volume shrinkage takes place when Sn reacts with Ni to form Ni_3Sn_4 IMC.[22] But we propose below a third reason which is unique due to the small solder volume.

In Fig. 2b, while there is a serious necking formation in the periphery of the solder joint, there is no void in the middle of the joint. We found that in Fig. 2b, the Ni_3Sn_4 IMCs on the top side and on the bottom side have not bridged together, thus the molten solder in the joint has the freedom to move or shrink in the direction normal to the interface of the solder joint. However, after the 34 min reflow, when the Ni_3Sn_4 IMCs on the both sides bridged together, large voids appeared in middle of the joint, as illustrated in Fig. 2c. This is because while the flow of molten solder is unlimited, the freedom of solder joint to shrink normal to its interface is limited. Thus, when the molten solder is drained by the side wall reaction, void must be formed in the middle of the solder joint. We will discuss the point later.

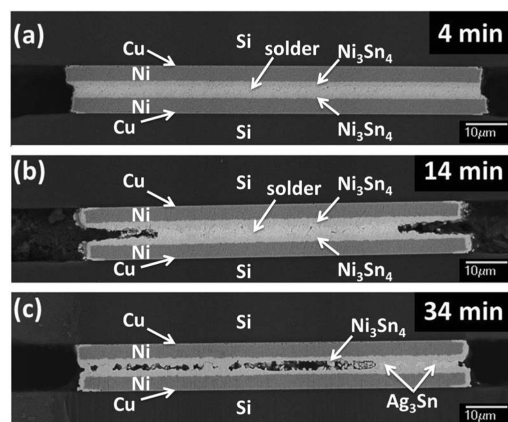

Figure 2. Cross-sectional SEM images showing the microbumps with 4-μm-thick solder subjected to a (a) 4 min (as-jointed); (b) 14 min; (c) 34 min reflow at 260°C.

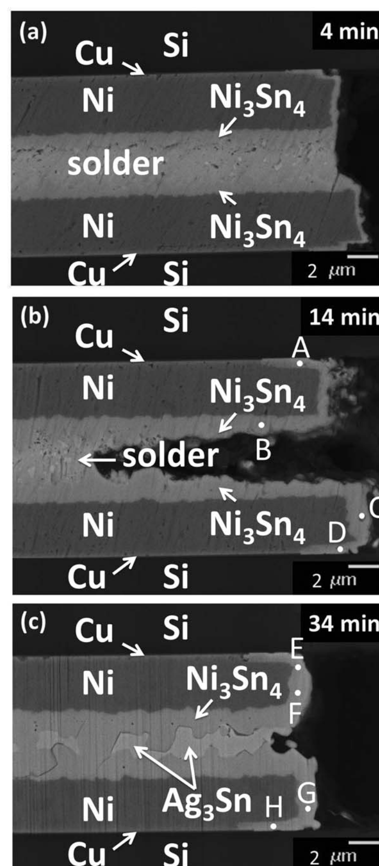

Figure 3. Enlarged cross-sectional SEM images showing the periphery of microbumps with 4-μm-thick solder after reflow for (a) 4 min (as-jointed); (b) 14 min; (c) 34 min at 260°C.

The locations for the Ag_3Sn precipitates appear differently at different stages. As shown in Figure 3a, finely-dispersed Ag_3Sn IMC can be observed in the solder matrix in the as-joined sample. After an additional 10 min reflow, as the solder gradually converted into Ni_3Sn_4 IMC, the Ni_3Sn_4 IMCs at the two interfaces thickened at about the same rate as shown in Figure 3b. The Ag_3Sn precipitates grew larger and they still distributed randomly in the solder matrix. However, when the reflowing time reached 34 min, the solder layer transformed completely into Ni_3Sn_4 IMC, as shown in Figure 3c, and some large Ag_3Sn IMC can be observed to appear near the edges of the microbump. This microbump was polished by FIB. Since the Ag atoms in the solder behaved as an inert element during the Sn/Ni interfacial reaction, they were constantly rejected and dissolved into the remaining molten solder during the Sn/Ni reaction. Eventually, all the Ag atoms precipitated out as the large Ag_3Sn IMC grains and they tend to adhere to Ni_3Sn_4 IMC. Therefore, the mechanical strength of the heterogeneous phase boundaries between Ag_3Sn and Ni_3Sn_4 is a key factor affecting the reliability of the microbumps in 3D IC applications.

As for the 11 μm thick solder microbumps, the side wall wetting and the necking formation at the periphery of the solder layer occurred at a much longer reflow time. As demonstrated in Figures 4a to 4d, the solder did not shrink obviously until the reflow time reached 64 min. When the reflow time reached 124 min, the morphology of the Ni_3Sn_4 grains became faceted as shown in Figure 4d.

As shown in Figure 2, it is intriguing that the necking located in the periphery of the microbumps for the 4 μm thick solder sample reflowed after 14 min. Yet, a large amount of voids scattered in the

Downloaded on 2014-04-28 to IP 140.113.38.11 address. Redistribution subject to ECS terms of use (see ecsdl.org/site/terms_use) unless CC License in place (see abstract).

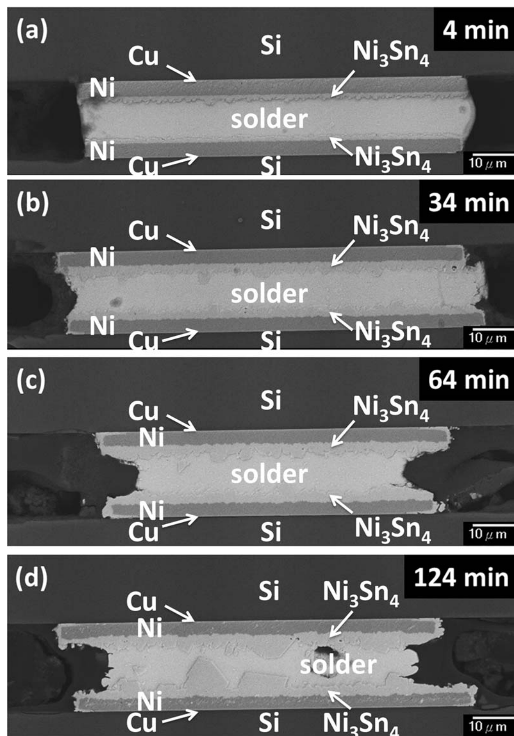

Figure 4. Cross-sectional SEM images showing the microbumps with 11-μm-thick solder after reflow for (a) 4 min (as-jointed); (b) 34 min; (c) 64 min; (d) 124 min at 260°C.

microbumps after reflowed of 34 min. This may be attributed to the following mechanism. Once the Ni_3Sn_4 IMCs bridged the joint; the physical height of the microbump is fixed. The joint cannot shrink anymore in the vertical direction. As the interfacial reaction continues, the molten solder becomes thinner. The molten solder may be drained much easier due to capillary force. As the molten solder is drained by side wall reaction, voids must form near the center region of the joint. For a larger and thicker solder joint, the IMC on the two sides of the joint will not be able to bridge each other, hence no void will form by this mechanism. Obviously, if we can prevent side wall reaction, no such kind of void formation will occur.

Conclusions

In summary, the interfacial reactions at 260°C in the Ni/Sn2.3Ag/Ni microbumps with 4 μm and 11 μm thick Sn2.3Ag solder have been studied. The effect of small solder thickness on void formation is significant. For the 4 μm thick solder, when the reflow time reached 14 min, serious necking or shrinking of the solder from the periphery was observed due to side wall wetting. After a 34 min reflow, voids formed in the center of the microbump. This is because the Ni_3Sn_4 IMCs from the upper and lower interface of the microbump have bridged together, it removed the degree of freedom of the microbump to move or to shrink in the normal direction. Hence a drain of the molten solder by the side wall wetting will leave voids in the center of the joint. This is a processing failure of the microbump in 3D IC applications. This is a unique mode of processing failure because of the smaller and smaller volume of solder joints in the trend of miniaturization. In the thicker 11 μm solder, it took much longer reflow time to allow the bridging of IMC.

Acknowledgment

The financial support from the National Science Council, Taiwan, under the contract NSC 98-2221-E-009-036-MY3, is acknowledged.

References

1. J. C. Lin, W. C. Chiou, K. F. Yang, H. B. Chang, Y. C. Lin, E. B. Liao, J. P. Hung, Y. L. Lin, P. H. Tsai, Y. C. Shih, T. J. Wu, W. J. Wu, F. W. Tsai, Y. H. Huang, T. Y. Wang, C. L. Yu, C. H. Chang, M. F. Chen, S. Y. Hou, C. H. Tung, S. O. Jeng, and D. C. H. Yu, in *Proceedings of International Electron Devices Meeting*, IEEE, 2.1.1 (2010).
2. K. N. Tu, *Microelectron. Reliab.*, **51**, 517 (2011).
3. K. N. Tu and K. Zeng, *Mater. Sci. Eng. R.*, **34**, 1 (2001).
4. P. G. Kim, J. W. Jang, T. Y. Lee, and K. N. Tu, *J. Appl. Phys.*, **86**, 6746 (1999).
5. M. He, A. Kumar, P. T. Yeo, G. J. Qi, and Z. Chen, *Thin Solid Films*, **462-463**, 387 (2004).
6. G. Ghosh, *J. Appl. Phys.*, **88**, 6887 (2000).
7. P. L. Tu, Y. C. Chan, K. C. Hung, and J. K. L. Lai, *Scr. Mater.*, **44**, 317 (2001).
8. G. Ghosh, *Acta Mater.*, **49**, 2609 (2011).
9. J. F. Li, S. H. Mannan, M. P. Clode, K. Chen, D. C. Whalley, C. Liu, and D. A. Hutt, *Acta Mater.*, **55**, 737 (2007).
10. G. Ghosh, *Acta Mater.*, **48**, 3719 (2000).
11. W. M. Tang, A. Q. He, Q. Liu, and D. G. Ivey, *Int. J. Miner. Metall. Mater.*, **17**, 459 (2010).
12. M. L. Huang, T. Loeher, D. Manessis, L. Boettcher, A. Ostmann, and H. Reichl, *J. Electron. Mater.*, **35**, 181 (2006).
13. S. J. Wang, H. J. Kao, and C. Y. Liu, *J. Electron. Mater.*, **33**, 1130 (2004).
14. R. Labie, W. Ruythooren, and J. V. Humbeeck, *Intermetallics*, **15**, 396 (2007).
15. W. J. Tomlinson and H. G. Rhodes, *J. Mater. Sci.*, **22**, 1769 (1987).
16. C. M. Chen and S. W. Chen, *Acta Mater.*, **50**, 2461 (2002).
17. M. O. Alam, Y. C. Chan, and K. C. Hung, *J. Electron. Mater.*, **31**, 1117 (2002).
18. J. W. Yoon, S. W. Kim, and S. B. Jung, *J. Alloys Compd.*, **385**, 192 (2004).
19. C. Y. Liu, H. W. Tseng, and J. M. Song, *Electrochem. Solid-State Lett.*, **13**, H298 (2010).
20. R. S. Cheng, H. J. Chang, T. C. Chang, and J. H. Chou, *Electrochem. Solid-State Lett.*, **15**, H75 (2012).
21. J. F. Li, P. A. Agyakwa, and C. M. Johnson, *Acta Mater.*, **59**, 1198 (2011).
22. H. Y. Chuang, J. J. Yu, M. S. Kuo, H. M. Tong, and C. R. Kao, *Scr. Mater.*, **66**, 171 (2012).
23. D. W. Zheng, W. Wen, and K. N. Tu, *Phys. Rev. E*, **57**, 3719 (1998).
24. C. Y. Liu and K. N. Tu, *Phys. Rev. E*, **58**, 6308 (1998).

Downloaded on 2014-04-28 to IP 140.113.38.11 address. Redistribution subject to ECS terms of use (see ecsdl.org/site/terms_use) unless CC License in place (see abstract).